Distribution of the spacing between two adjacent avoided crossings

Manabu Machida[1,*] and Keiji Saito[2,†]

[1]*Institute of Industrial Science, The University of Tokyo, Meguro-ku, Tokyo 153-8505, Japan*
[2]*Department of Physics, Graduate School of Science, The University of Tokyo, Bunkyo-ku, Tokyo 113-0033, Japan*
(Received 29 July 2005; published 11 November 2005)

We consider the frequency at which avoided crossings appear in an energy-level structure when an external field is applied to a quantum chaotic system. The distribution of the spacing in the parameter between two adjacent avoided crossings is investigated. Using a random matrix model, we find that the distribution of these spacings is well fitted by a power-law distribution for small spacings. The powers are 2 and 3 for the Gaussian orthogonal ensemble and Gaussian unitary ensemble, respectively. We also find that the distributions decay exponentially for large spacings. The distributions in concrete quantum chaotic systems agree with those of the random matrix model.

PACS number(s): 05.45.Mt

I. INTRODUCTION

The avoided crossing is a ubiquitous structure in energy levels of quantum chaotic systems with external perturbation [1]. As the time-dependent external perturbation is applied to the system, the quantum state changes nonadiabatically. Especially when the perturbation changes linearly and slowly in time, nonadiabatic transitions can be described by the Landau-Zener transitions [2] at avoided crossings. Using this microscopic mechanism, the nonadiabatic change of the total quantum state might be understood. Energy diffusion phenomena have been intensively studied from this point of view [3–6]. To understand macroscopic phenomena such as energy diffusion, it is important to study universal aspects of avoided crossings in quantum systems. Thus, using random matrices [7,8], various distributions concerning avoided crossings have been studied [9]. For example, the distributions of the energy-level curvature [10–14], the difference between the slopes of the asymptotic lines [15,16], and the minimum-energy gap [16,17] are derived at avoided crossings, and their universalities are confirmed in concrete quantum systems [11,12,16–18].

In this paper, we consider another distribution related to the structure of avoided crossings. We study the distribution of the spacing in a parameter space of perturbation, which is measured as the distance between two adjacent avoided crossings involved in two neighboring energy levels (examples of this spacing are depicted in Fig. 1). We call this distribution the avoided-crossing spacing distribution (ACSD). Only a few qualitative studies related to the ACSD have been published. Goldberg and Schweizer obtained the ACSD of the hydrogen atom in a magnetic field and that of the Africa billiard to estimate the statistical error of the gap distribution [19]. Wilkinson and Austin discussed the density of avoided crossings in quantum systems with two free parameters, although the distribution of the spacing between avoided crossings was not discussed [20]. The main aim of

this paper is to obtain the *quantitative* properties of the ACSD.

We first consider the Hamiltonian taken from random matrices to extract the general features of the ACSD. We calculate the ACSD's for the Gaussian orthogonal ensemble (GOE) and the Gaussian unitary ensemble (GUE) by a precise numerical calculation. We find that, for small spacings, the ACSD for the GOE (GUE) shows a power-law behavior with power 2 (3). For large spacings, the ACSD's decay exponentially. We then consider two concrete quantum systems—i.e., the coupled rotators model and the Aharonov-Bohm billiard—and find that the ACSD's of these systems agree with those predicted by simulations using random matrices.

This paper is constructed as follows. In Sec. II, we obtain the ACSD's of a random matrix model for the GOE and GUE, and discuss differences between them, focusing especially on the powers of the distributions. In Secs. III and IV, we present the ACSD's of two concrete models and show that they are identical to those of the corresponding random matrix models. Finally, in Sec. V, we give a summary.

II. RANDOM MATRIX MODEL

Let us consider an $N \times N$ Hamiltonian matrix $\mathcal{H}(\Lambda)$ including a parameter Λ as an external field. In order to cap-
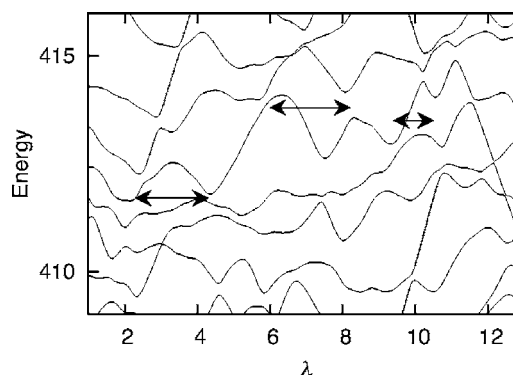

FIG. 1. The scaled energy spectrum for $\mathcal{H}_{RM}(\Lambda)$ of the GOE as a function of λ. Three examples of avoided-crossing spacings are also shown.

---

*Electronic address: machida@iis.u-tokyo.ac.jp
†Electronic address: saitoh@ap.t.u-tokyo.ac.jp

ture general features of the ACSD, we take $\mathcal{H}(\Lambda)$ from random matrix ensembles [1,7]. We prepare random matrices $\mathcal{H}_0^{\mathrm{RM}}$ and $\mathcal{V}^{\mathrm{RM}}$ of $N=1000$. We consider the following random matrix model:

$$\mathcal{H}_{\mathrm{RM}}(\Lambda) = \mathcal{H}_0^{\mathrm{RM}} \cos \Lambda + \mathcal{V}^{\mathrm{RM}} \sin \Lambda. \quad (1)$$

Note that this model keeps the variance of matrix elements unchanged as the parameter varies [16].

If we take both $\mathcal{H}_0^{\mathrm{RM}}$ and $\mathcal{V}^{\mathrm{RM}}$ from the GOE, the Hamiltonian $\mathcal{H}_{\mathrm{RM}}(\Lambda)$ represents quantum systems invariant under an antiunitary transformation such as the time-reversal transformation. On the other hand, if we take both of them from the GUE, the Hamiltonian represents quantum systems that have no symmetries for antiunitary transformations [1,8,21]. We let Λ move from 0.5 to 1.5. The variance σ_{RM}^2 of diagonal elements of $\mathcal{H}_0^{\mathrm{RM}}$ and $\mathcal{V}^{\mathrm{RM}}$ is 2.

First of all, we need to scale Λ and $E_j(\Lambda)$ [the jth eigenvalue of the instantaneous Hamiltonian $\mathcal{H}(\Lambda)$] in order to eliminate the dependence of the parameters on the external field and energy [22–26]. Following Simons and Altshuler [22], we define the scaled parameter λ and scaled energy ϵ_j as

$$\epsilon_j(\Lambda) = \epsilon_1(\Lambda) + \sum_{i=1}^{j-1} \frac{E_{i+1}(\Lambda) - E_i(\Lambda)}{\Delta_i(\Lambda)},$$

$$\lambda_{kj} = \lambda_{0j} + \sum_{k'=1}^{k-1} (\Lambda_{k'+1} - \Lambda_{k'}) \sqrt{\left\langle \left(\left. \frac{\partial \epsilon_j(\Lambda)}{\partial \Lambda} \right|_{\Lambda_{k'}} \right)^2 \right\rangle}, \quad (2)$$

where $\Delta_j(\Lambda)$ is the mean level spacing at $E_j(\Lambda)$ and $\langle \cdots \rangle$ denotes a statistical average over a typical range of levels and Λ. We put $\epsilon_1(\Lambda)=0 (=\mathrm{const})$, which is followed by $\langle \partial \epsilon_j(\Lambda)/\partial \Lambda \rangle = 0$. λ_{0j} is set to Λ_0. Thus, we obtain the scaled energy level flow $\epsilon_j(\lambda)$. We show the scaled energy spectrum $\epsilon_j(\lambda)$ for $\mathcal{H}_{\mathrm{RM}}(\Lambda)$ of the GOE in Fig. 1. Some avoided crossings look like crossings indeed, but this is due solely to the linewidth. In Fig. 1, three distances (the right and left arrows) are shown as examples of avoided-crossing spacing.

An avoided-crossing spacing is defined by the spacing between two neighboring avoided crossings on the same energy level flow. Now, λ_{kj} is identified as the position of an avoided crossing on the jth energy level flow if $\epsilon_{j+1}(\lambda_{k-1,j+1}) - \epsilon_j(\lambda_{k-1,j}) > \epsilon_{j+1}(\lambda_{k,j+1}) - \epsilon_j(\lambda_{k,j})$ and $\epsilon_{j+1}(\lambda_{k+1,j+1}) - \epsilon_j(\lambda_{k+1,j}) > \epsilon_{j+1}(\lambda_{k,j+1}) - \epsilon_j(\lambda_{k,j})$ are satisfied. By taking the differences in positions between two adjacent avoided crossings, avoided-crossing spacings S_λ are obtained. We thereby obtain the ACSD $P(S_\lambda)$—i.e., the probability that the spacing in the parameter space of the adjacent avoided crossings is S_λ. Here $P(S_\lambda)$ satisfies the following normalization conditions:

$$\int_0^\infty P(S_\lambda) dS_\lambda = 1, \quad \int_0^\infty S_\lambda P(S_\lambda) dS_\lambda = 1. \quad (3)$$
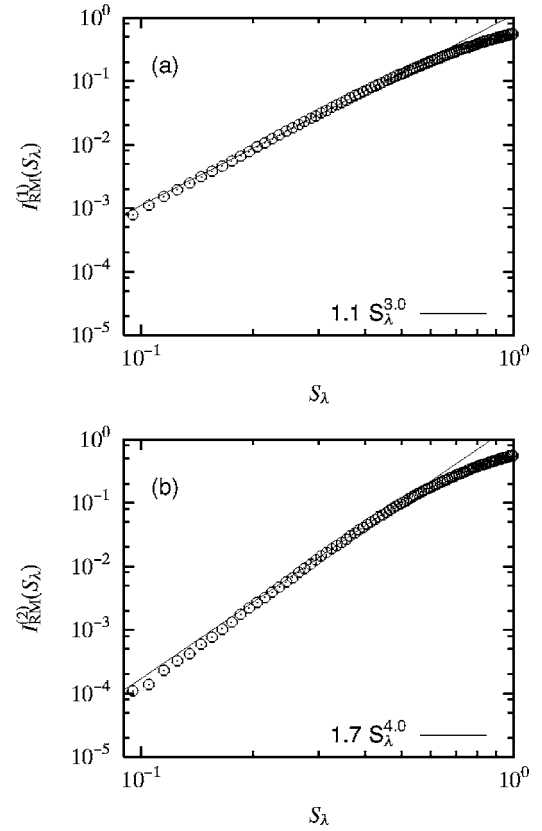

FIG. 2. Log-log plots of the cumulative distributions (a) $I_{\mathrm{RM}}^{(1)}(S_\lambda)$ and (b) $I_{\mathrm{RM}}^{(2)}(S_\lambda)$.

Hereafter, we distinguish between the GOE and GUE by the superscript β. We have $\beta=1$ for the GOE and $\beta=2$ for the GUE. That is, $P_{\mathrm{RM}}^{(\beta)}(S_\lambda)$ denotes the ACSD of model (1) for the GOE and GUE. We take the parameter slice $\Delta\Lambda \equiv \Lambda_{k+1} - \Lambda_k$ to be 0.001, which is small enough. We find 4.0×10^5 (3.5×10^5) avoided-crossing spacings in 50 samples of $\mathcal{H}_{\mathrm{RM}}(S_\lambda)$ for the GOE (GUE).

We also define the cumulative distribution $I_{\mathrm{RM}}^{(\beta)}(S_\lambda)$ of the ACSD of $\mathcal{H}_{\mathrm{RM}}(\lambda)$ for the GOE and GUE as $I_{\mathrm{RM}}^{(\beta)}(S_\lambda) = \int_0^{S_\lambda} P_{\mathrm{RM}}^{(\beta)}(S'_\lambda) dS'_\lambda$. Figure 2 shows log-log plots of $I_{\mathrm{RM}}^{(\beta)}(S_\lambda)$. The solid lines in the figures are obtained by fitting the data in the small-S_λ region by the least-squares method. Consequently, we find that $I_{\mathrm{RM}}^{(1)}(S_\lambda)$ behaves as $1.1 \times S_\lambda^{3.0}$ and that $I_{\mathrm{RM}}^{(2)}(S_\lambda)$ behaves as $1.7 \times S_\lambda^{4.0}$. Therefore, we may write

$$P_{\mathrm{RM}}^{(\beta)}(S_\lambda) \sim S_\lambda^{\beta+1} \quad (S_\lambda \ll 1). \quad (4)$$

To study how the ACSD decays, we compare $P_{\mathrm{RM}}^{(\beta)}(S_\lambda)$ with the following trial function:

$$P_{\mathrm{trial}}^{(\beta)}(S_\lambda) = \frac{a_\beta S_\lambda^{\beta+2}}{\sinh b_\beta S_\lambda}. \quad (5)$$

Here, the coefficients a_β and b_β are determined from the normalization conditions (3): $a_1 = (8/\pi^4) b_1^4$, $b_1 = 372\zeta(5)/\pi^4$, $a_2 = [2/93\zeta(5)] b_2^5$, and $b_2 = \pi^6/186\zeta(5)$. In Figs. 3(a) and 3(b), we see that $P_{\mathrm{RM}}^{(\beta)}(S_\lambda)$ is well approximated by $P_{\mathrm{trial}}^{(\beta)}(S_\lambda)$ for large S_λ. Since Eq. (5) implies that $P_{\mathrm{RM}}^{(\beta)}(S_\lambda)$ decays ex-
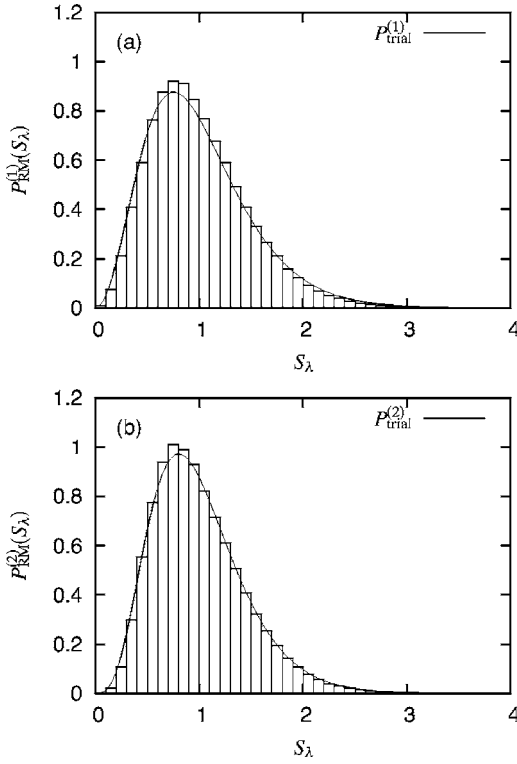
FIG. 3. (a) For $\beta=1$, $P_{RM}^{(\beta)}(S_\lambda)$ is compared with $P_{trial}^{(\beta)}(S_\lambda)$. (b) The same as (a) except $\beta=2$.

FIG. 4. (a) Histogram of $P_{CRT}(S_\lambda)$ with $P_{RM}^{(1)}(S_\lambda)$. (b) $I_{CRT}(S_\lambda)$ together with $I_{RM}^{(1)}(S_\lambda)$ and $I_{RM}^{(2)}(S_\lambda)$. The inset shows the magnified figure with a log-log plot near the origin.

ponentially for large S_λ, we may conclude that no correlation exists between avoided crossings for large S_λ. Note that, for small S_λ, we have $P_{trial}^{(1)}(S_\lambda) \simeq 5.1 S_\lambda^2$ and $P_{trial}^{(2)}(S_\lambda) \simeq 64 S_\lambda^3$, which do not reproduce the numerical data.

We also obtained the ACSD of the following random matrix Hamiltonian:

$$\mathcal{H}_{RM0}(\Lambda) = \mathcal{H}_0^{RM} + \Lambda \mathcal{V}^{RM}. \qquad (6)$$

We checked that the ACSD of this model is the same as that of $\mathcal{H}_{RM}(\Lambda)$ in Eq. (1).

III. COUPLED ROTATORS MODEL

As an example of quantum systems for the GOE, we consider the coupled-rotators model [27]. We shall show that the ACSD of this model is well approximated by $P_{RM}^{(1)}(S_\lambda)$. The Hamiltonian of the system is given by

$$\mathcal{H}_{CRT}(\Lambda) = L_1^x L_2^x + \Lambda(L_1^z + L_2^z), \qquad (7)$$

where L_1 and L_2 are angular momenta with l_1 and l_2—i.e., the eigenvalues of L_1^2 and L_2^2 are $l_1(l_1+1)\hbar^2$ and $l_2(l_2+1)\hbar^2$, respectively. Since $\hbar$ is a dimensionless parameter in the present unit, we put $\hbar=0.158\,75$ so that the corresponding classical system becomes strongly chaotic [28]. Noting that $\mathcal{H}_{CRT}(\Lambda)$ changes the z component of the total angular momentum ($J^z=L_1^z+L_2^z$) by 0, $\pm 2\hbar$ [29], the Hilbert space is divided into two subspaces corresponding to even $J^z/\hbar$ and odd $J^z/\hbar$. Here, we take the subspace in which $J^z/\hbar$ is even. Furthermore, we divide this subspace into two more sub-
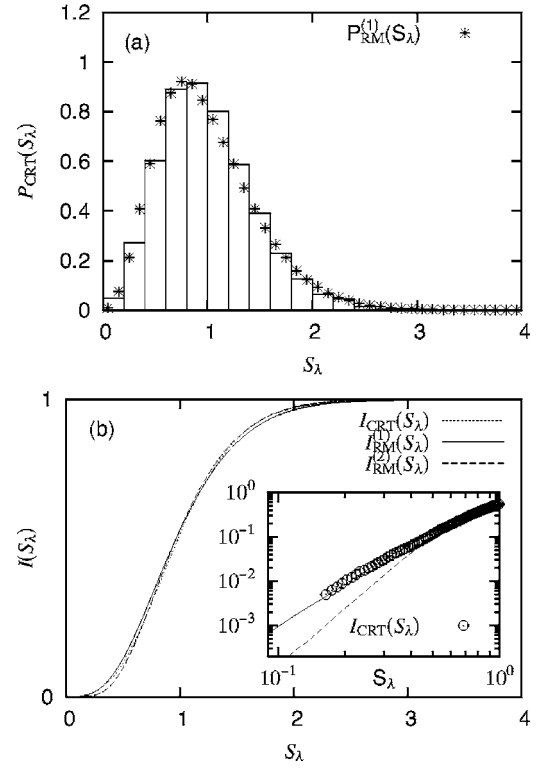
spaces corresponding to the states symmetric and antisymmetric under the exchange of L_1^z and L_2^z. Here, we choose the subspace corresponding to the symmetric states. In this subspace, we have 1024 levels with no degeneracies when we set $l_1=l_2=31$. We have confirmed that the energy-level spacing distribution of the coupled rotators model is well approximated by the eigenvalue distribution of random matrices taken from the GOE in the whole range of $\Lambda \in [0.5, 1.5]$.

After the scaling (2), we find 9094 avoided-crossing spacings. Thus, we obtain the ACSD of the coupled-rotators model $P_{CRT}(S_\lambda)$ and the cumulative distribution $I_{CRT}(S_\lambda)$ $\times[=\int_0^{S_\lambda} P_{CRT}(S_\lambda')dS_\lambda']$. In Fig. 4(a), we show $P_{CRT}(S_\lambda)$ together with $P_{RM}^{(1)}(S_\lambda)$. We see that $P_{CRT}(S_\lambda)$ is roughly equal to $P_{RM}^{(1)}(S_\lambda)$. In Fig. 4(b), we show $I_{CRT}(S_\lambda)$ with $I_{RM}^{(1)}(S_\lambda)$ and $I_{RM}^{(2)}(S_\lambda)$. The inset, which shows the magnified figure with a log-log plot, shows that $I_{CRT}(S_\lambda)$ follows $I_{RM}^{(1)}(S_\lambda)$. Therefore, we classify $P_{CRT}(S_\lambda)$ as $P_{RM}^{(1)}(S_\lambda)$.

IV. AHARONOV-BOHM BILLIARD

Now we consider the Aharonov-Bohm billiard as an example of a quantum system corresponding to the GUE [30–32]. We shall show that the ACSD of this system is well approximated by $P_{RM}^{(2)}(S_\lambda)$. In the billiard, a charged particle with mass m and charge q moves inside the boundary ∂D. The domain D is threaded by a magnetic flux Φ at the origin. The Schrödinger equation of this system is written as
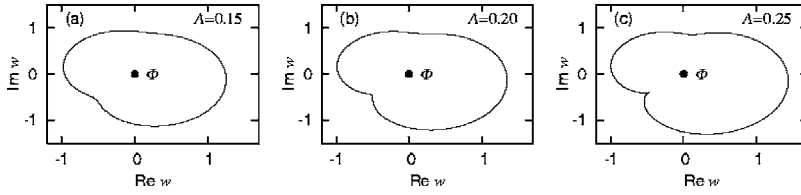
FIG. 5. Boundaries of the Aharonov-Bohm billiard with $\Lambda=$ (a) 0.15, (b) 0.2, and (c) 0.25.

$$\frac{1}{2m}[-i\hbar\boldsymbol{\nabla}_{uv} - q\boldsymbol{A}(r)]^2\psi(r) = E\psi(r)$$

$$\boldsymbol{\nabla}_{uv} \times \boldsymbol{A}(r) = \hat{\boldsymbol{n}}\Phi\delta(u)\delta(v), \tag{8}$$

where $\boldsymbol{r}=(u,v)$, $\psi(r)=0$ on ∂D, and $\hat{\boldsymbol{n}}$ is the unit vector perpendicular to the billiard. The domain D is determined by the following conformal transformation in the complex plane $w=u+iv$:

$$w = z + \Lambda z^2 + \Lambda e^{i\pi/3}z^3. \tag{9}$$

Here, $z(=x+iy)$ is a complex value in the unit disk ($|z|\leqslant 1$). The parameter Λ determines the shape of the billiard. Figure 5 shows the boundaries of the billiard when $\Lambda=0.15$, 0.2, and 0.25.

Let us introduce two new parameters:

$$\alpha \equiv \frac{q\Phi}{2\pi\hbar}, \quad k^2 \equiv \frac{2mE}{\hbar}. \tag{10}$$

The value of α is restricted to the range $\left[0,\frac{1}{2}\right]$ from the symmetry of the system [30]. We put $\alpha=\frac{1}{4}$, with which the corresponding classical system becomes most strongly chaotic [30]. Now, the problem with getting the energy E of the system in the Schrödinger equation (8) results in the following eigenvalue problem by expanding the wave function with the Bessel function [30]:

$$\sum_{n'l'} c_{n'l'}M_{n'l'nl}(\Lambda) = \frac{c_{nl}}{k^2}. \tag{11}$$

Here, $\{c_{nl}\}$ are components of the eigenvectors and

$$M_{n'l'nl}(\Lambda) = \frac{N_{nl}N_{n'l'}}{a_{nl}a_{n'l'}}\int_0^1 dr r \int_0^{2\pi} d\phi e^{i(l-l')\phi}J_{|l-\alpha|}(a_{nl}r)J_{|l'-\alpha|}$$
$$\times (a_{n'l'}r)|w'(z)|^2, \tag{12}$$

where a_{nl} is the nth zero of the Bessel function $J_{|l-\alpha|}(x)$ and

$$N_{nl} = \frac{1}{\sqrt{\pi}}|J'_{|l-\alpha|}(a_{nl})|^{-1}. \tag{13}$$

Thus, we obtain the energy eigenvalues of the system by diagonalizing the Hermitian matrix $M(\Lambda)$.

We make a 2000×2000 matrix as $M(\Lambda)$ and use the lowest 550 levels [31]. We have confirmed that the energy-level spacing distribution of the system is well approximated by the eigenvalue distribution of the GUE in the whole range of $\Lambda \in [0.15,0.25]$.

After the scaling (2), we find 1050 avoided-crossing spacings. Thus, we obtain the ACSD of the Aharonov-Bohm billiard $P_{AB}(S_\lambda)$ and the cumulative distribution $I_{AB}(S_\lambda)$

$\times[=\int_0^{S_\lambda}P_{AB}(S'_\lambda)dS'_\lambda]$. In Fig. 6(a), we show $P_{AB}(S_\lambda)$ together with $P_{RM}^{(2)}(S_\lambda)$. We see that $P_{AB}(S_\lambda)$ is roughly equal to $P_{RM}^{(2)}(S_\lambda)$. In Fig. 6(b), we show $I_{AB}(S_\lambda)$ with $I_{RM}^{(1)}(S_\lambda)$ and $I_{RM}^{(2)}(S_\lambda)$. The inset, which shows the magnified figure with a log-log plot, reveals that $I_{AB}(S_\lambda)$ follows $I_{RM}^{(2)}(S_\lambda)$. Therefore, we conclude that the ACSD of the Aharonov-Bohm billiard is classified as $P_{RM}^{(2)}(S_\lambda)$.

V. SUMMARY

We have studied the ACSD in quantum chaotic systems. The distribution $P_{RM}^{(\beta)}(S_\lambda)$ of the random matrix model was numerically obtained. We found power-law behavior for small spacings and exponential decay for large spacings. For small spacings, we found that the powers for the GOE and GUE are 2 and 3, respectively. The exponential decay implies that the correlation between two avoided crossings vanishes for large spacings. Although these properties are established numerically, an analytical proof for them remains to be completed. In Secs. III and IV, we have shown by accurate numerical calculations that the distributions predicted by
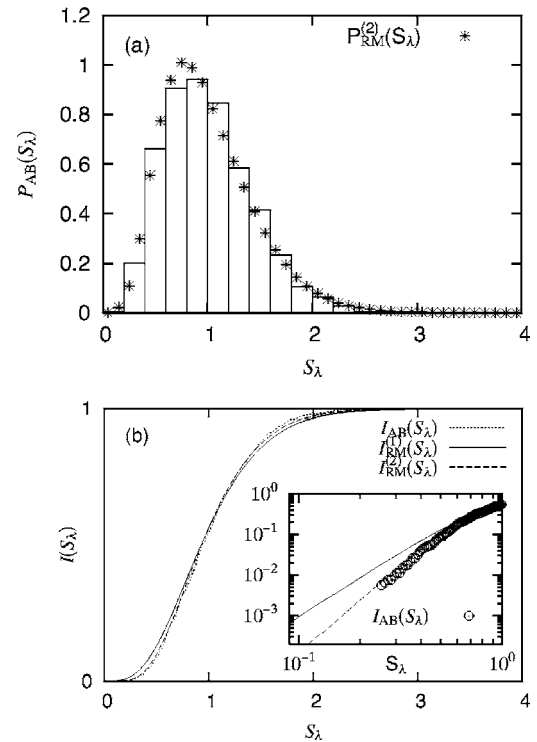

FIG. 6. (a) Histogram of $P_{AB}(S_\lambda)$ with $P_{RM}^{(2)}(S_\lambda)$. (b) $I_{AB}(S_\lambda)$ together with $I_{RM}^{(1)}(S_\lambda)$ and $I_{RM}^{(2)}(S_\lambda)$. The inset shows the magnified figure with a log-log plot near the origin.

the random matrix model are indeed realized in concrete quantum chaotic systems.

The ACSD may play an important role in the quantum dynamics of finite fermion systems such as quantum billiards [4]. It is especially worthwhile to consider the time duration until the system starts diffusing after the external perturbation is applied at zero temperature. As the perturbation is applied, pairs of neighboring levels in the energy level flow form avoided crossings. The quantum state at the Fermi level changes over time by making a nonadiabatic transition at the avoided crossing. The distribution of the time duration until the Fermi level encounters the first avoided crossing would be related to the ACSD. It is interesting to experimentally observe the time duration and to understand it in the context of the ACSD.

[1] F. Haake, *Quantum Signatures of Chaos*, 2nd ed. (Springer, Berlin, 2001).

[2] L. Landau, Phys. Z. Sowjetunion **2**, 46 (1932); C. Zener, Proc. R. Soc. London, Ser. A **137**, 696 (1932).

[3] Y. Gefen and D. J. Thouless, Phys. Rev. Lett. **59**, 1752 (1987).

[4] M. Wilkinson, J. Phys. A **21**, 4021 (1988).

[5] M. Wilkinson, Phys. Rev. A **41**, 4645 (1990).

[6] M. Machida, K. Saito, and S. Miyashita, J. Phys. Soc. Jpn. **71**, 2427 (2002).

[7] M. L. Mehta, *Random Matrices* (Academic, San Diego, CA, 1991).

[8] C. E. Porter, *Statistical Theories of Spectra: Fluctuations* (Academic Press, London, 1965).

[9] T. Guhr, A. Müller-Groeling, and A. Weidenmüller, Phys. Rep. **299**, 189 (1998).

[10] P. Gaspard, S. A. Rice, and K. Nakamura, Phys. Rev. Lett. **63**, 930 (1989).

[11] P. Gaspard, S. A. Rice, H. J. Mikeska, and K. Nakamura, Phys. Rev. A **42**, 4015 (1990).

[12] J. Zakrzewski and D. Delande, Phys. Rev. E **47**, 1650 (1993).

[13] F. von Oppen, Phys. Rev. Lett. **73**, 798 (1994).

[14] F. von Oppen, Phys. Rev. E **51**, 2647 (1995).

[15] M. Wilkinson, J. Phys. A **22**, 2795 (1989).

[16] J. Zakrzewski, D. Delande, and M. Kuś, Phys. Rev. E **47**, 1665 (1993).

[17] J. Zakrzewski and M. Kuś, Phys. Rev. Lett. **67**, 2749 (1991).

[18] T. Takami and H. Hasegawa, Phys. Rev. Lett. **68**, 419 (1992).

[19] J. Goldberg and W. Schweizer, J. Phys. A **24**, 2785 (1991).

[20] M. Wilkinson and E. J. Austin, Phys. Rev. A **47**, 2601 (1993).

[21] O. Bohigas, M. J. Giannoni, and C. Schmit, Phys. Rev. Lett. **52**, 1 (1984).

[22] B. D. Simons and B. L. Altshuler, Phys. Rev. Lett. **70**, 4063 (1993).

[23] B. D. Simons, A. Szafer, and B. L. Altshuler, JETP Lett. **57**, 276 (1993).

[24] B. D. Simons and B. L. Altshuler, Phys. Rev. B **48**, 5422 (1993).

[25] Y. Alhassid and H. Attias, Phys. Rev. Lett. **74**, 4635 (1995).

[26] H. Attias and Y. Alhassid, Phys. Rev. E **52**, 4776 (1995).

[27] M. Feingold and A. Peres, Physica D **9**, 433 (1983).

[28] M. Feingold, N. Moiseyev, and A. Peres, Phys. Rev. A **30**, 509 (1984).

[29] F. Borgonovi, I. Guarneri, and F. M. Izrailev, Phys. Rev. E **57**, 5291 (1998).

[30] M. V. Berry and M. Robnik, J. Phys. A **19**, 649 (1986).

[31] M. Robnik, J. Phys. A **25**, 1399 (1992).

[32] M. Robnik, J. Dobnikar, and T. Prosen, J. Phys. A **32**, 1427 (1999).